$[^{98}MoO(SePh)_4]^-$ and $[^{98}MoOCl_4(MeCN)]^-$ enriched with 24.9 atom % ^{17}O, presumably due to their intrinsically broader line widths (Table VI) and insufficient enrichment. The observation[34,35] of ^{17}O superhyperfine coupling of about $(8–16) \times 10^{-4}$ cm^{-1} in the molybdoenzymes xanthine oxidase, xanthine dehydrogenase, and sulfite oxidase in $^{17}OH_2$ demonstrates the presence of an exchangeable oxygen in the molybdenum coordination sphere. The magnitude of the coupling constants suggest that the exchangeable oxygen is an "in-plane" rather than an "axial" ligand.

Acknowledgment. Dr. J. R. Pilbrow and Dr. A. Edgar are thanked for their provision of computer simulation procedures and Q-band frequency measurements, respectively. A.G.W. thanks the Australian Research Grants Committee for financial support while G.R.H. acknowledges the award of a La Trobe University Postgraduate scholarship. K.S.M. acknowledges support from the Australian Research Grants Committee and a Monash University Special Research Grant. The assistance of Messrs. K. J. Berry and L. Mitchell with magnetic susceptibility measurements is gratefully acknowledged.

(34) Gutteridge, S.; Malthouse, J. P. G.; Bray, R. C. *J. Inorg. Biochem.* **1979**, *11*, 355–360.
(35) Cramer, S. P.; Johnson, J. L.; Rajagopalan, K. V.; Sorrell, T. M. *Biochem. Biophys. Res. Commun.* **1979**, *91*, 434–439.

Redox Properties of Thiolate Compounds of Oxomolybdenum(V) and Their Tungsten and Selenium Analogues

Julie R. Bradbury, Anthony F. Masters, Angus C. McDonell, Andrew A. Brunette, Alan M. Bond,*[1] and Anthony G. Wedd*

Contribution from the Department of Inorganic and Analytical Chemistry, La Trobe University, Bundoora, 3083, Australia, and the Division of Chemical and Physical Sciences, Deakin University, Waurn Ponds, 3217, Australia. *Received July 22, 1980*

Abstract: The rich electrochemistry of the mononuclear $[M^VO(XR)_4]^-$ and triply bridged binuclear $[M^V_2O_2(XR)_6Z]^{n-}$ anions (M = Mo, W; X = S, Se; R = Ph, *p*-tolyl, CH_2Ph; Z = uninegative ($n = 1$) or neutral ($n = 0$) ligand) is explored in MeCN and DMF at platinum and mercury electrodes over the temperature range +25 to −60 °C. Interconversion of the mononuclear and binuclear forms occurs via reduction and oxidation processes involving the metal and ligand centers. Stepwise reduction of the binuclear M^V_2 to $M^{IV,V}_2$ and M^{IV}_2 species is observed, and the reduced forms undergo chemical reactions which lead to the appearance of 1 molecule of $[M^{IV}O(XR)_4]^{2-}$/molecule of $[M^V_2O_2(XR)_6Z]^-$ reduced. In this way, the alkyl-substituted $[MoO(SCH_2Ph)_4]^{2-/-}$ ions can be generated at 25 °C. Chemically reversible, one-electron reduction of $[M^VO(XR)_4]^-$ is observed, while oxidation leads to the formation of $[M^V_2O_2(XR)_6Z]$ (Z = solvent) and RXXR via a process involving oxidative dissociation of ligand XR^-. For $[W^VO(XR)_4]^-$, the following one-electron couples are observed: $[W^{VI}O(XR)_4] + e^- = [W^VO(XR)_4]^-$ + $e^- = [W^{IV}O(XR)_4]^{2-}$. In view of the direct observation of $[W^{VI}O(XR)_4]$, an intramolecular redox step is apparently involved in the overall oxidation process described above. Wider implications of the ligand redox processes are discussed.

The molybdenum centers in the redox enzymes sulfite oxidase, xanthine oxidase and dehydrogenase, aldehyde oxidase, and nitrate reductase appear to cycle between the oxidation states VI, V, and IV during enzyme turnover[2] and, at least for sulfite oxidase and xanthine oxidase,[3] involve oxo and sulfur ligands. The present paper explores the rich redox chemistry of the mononuclear $[M^VO(XR)_4]^-$ (I) and triply bridged binuclear $[M^V_2O_2(XR)_6Z]^-$ (II) anions (M = Mo, W; X = S, Se; R = Ph, *p*-tolyl, CH_2Ph; Z = uninegative ligand) whose synthesis and electronic properties were described in the preceding paper.[4] The participation of thiolate ligand redox processes in the complex electrochemistry of these species is a significant observation. Preliminary redox aspects of the molybdenum–thiolate systems have been previously communicated.[5] The availability of the tungsten and selenium analogues permits a most detailed examination of the system.

Recent work[6–14] has considered the electrochemistry of various mono- and binuclear molybdenum complexes and, in particular, of compounds[11–14] of oxomolybdenum(V) containing multidentate thiolate ligands (including cysteine and its ethyl ester).

Experimental Section

All solution manipulations were carried out under purified argon or dinitrogen with use of standard techniques. Compounds were synthesized as described previously.[4,15,16]

Electrochemistry. The techniques employed were dc polarography at a dropping mercury electrode (dme), cyclic voltammetry (CV) at a

(1) Deakin University.
(2) Coughlan, M. P., Ed. "Molybdenum-Containing Enzymes"; Pergamon Press: Oxford, 1979.
(3) (a) Cramer, S. P.; Gray, H. B.; Rajagopalan, K. V. *J. Am. Chem. Soc.* **1979**, *101*, 2772–2774. (b) Tullius, T. D.; Kurtz, S. M.; Conradson, S. D.; Hodgson, K. O. *Ibid.* 2776–2779. (c) Bordas, J.; Bray, R. C.; Garner, C. D.; Gutteridge, S.; Hasnain, S. S. *J. Inorg. Biochem.* **1979**, *11*, 181–186.
(4) Hanson, G. R.; Brunette, A. A.; McDonell, A. C.; Murray, K. S.; Wedd, A. G. *J. Am. Chem. Soc.*, preceding paper in this issue.
(5) Bradbury, J. R.; Wedd, A. G.; Bond, A. M. *J. Chem. Soc., Chem. Commun.* **1979**, 1022–1025.
(6) Chalilpoyil, P.; Anson, F. C. *Inorg. Chem.* **1978**, *17*, 2418–2423.
(7) Lamache-Duhameaux, M. *J. Less-Common Met.* **1977**, *54*, 90.
(8) Wilshire, J. P.; Leon, L.; Bosserman, P.; Sawyer, D. T. *J. Am. Chem. Soc.* **1979**, *101*, 3379–3381.
(9) Hyde, J.; Venkatasubramanian, K.; Zubieta, J. *Inorg. Chem.* **1978**, *17*, 414–426.
(10) Schultz, F. A.; Ott, V. R.; Rolison, D. S.; Bravard, D. C.; McDonald, J. W.; Newton, W. E. *Inorg. Chem.* **1978**, *17*, 1758–1765.
(11) Ott, V. R.; Sweeter, D. S.; Schultz, F. A. *Inorg. Chem.* **1977**, *16*, 2538–2545.
(12) Howie, J. K.; Sawyer, D. T. *Inorg. Chem.* **1976**, *15*, 1892–1899.
(13) Bunzey, G.; Enemark, J. H.; Howie, J. K.; Sawyer, D. T. *J. Am. Chem. Soc.* **1977**, *99*, 4168–4170.
(14) Taylor, R. D.; Street, J. P.; Minelli, M.; Spence, J. T. *Inorg. Chem.* **1978**, *17*, 3207–3211.
(15) Boyd, I. W.; Dance, I. G.; Murray, K. S.; Wedd, A. G. *Aust. J. Chem.* **1978**, *31*, 279–284.
(16) Boyd, I. W.; Dance, I. G.; Landers, A. E.; Wedd, A. G. *Inorg. Chem.* **1979**, *18*, 1875–1885.

0002-7863/81/1503-1959$01.25/0

Table I. Redox Processes Occurring in 10^{-3} M Solutions of HXR, $[XR]^-$, and RXXR in DMF and MeCN at 25 °C

		peak potentials,[a] V						
		MeCN vs. $Ag/AgNO_3$ (0.1 M)			DMF vs. SCE			
peak no.	redox process	SPh	S-*p*-tolyl	SCH_2Ph[b]	SPh	S-*p*-tolyl	SCH_2Ph	SePh
1	$2HXR + 2e^- \rightarrow 2[XR]^- + H_2$	−1.90	−1.86	−2.28	−1.40	−1.50	−2.0	−1.15
2	$RXXR + 2e^- \rightarrow 2[XR]^-$	−2.20	−2.22	−2.30	−1.75	−1.7	−2.33	−1.20
1′	$2[XR]^- + H_2 \rightarrow 2HXR + 2e^-$	−0.1[c]		+0.3[c]	−0.45	−0.4[c]	−0.03	+0.35
2′	$2[XR]^- \rightarrow RXXR + 2e^-$	−0.31	−0.39	−0.2[c]	+0.03	−0.04	−0.3	−0.35
3′	$2HXR \rightarrow RXXR + 2H^+ + 2e^-$	+0.6[c]	+1.0[c]		+0.9	+1.4	+1.5	+1.0
4′	$RXXR \rightarrow [RXXR]^{+\cdot} + e^-$	+1.4	+1.3	+1.5				+1.6
5	$2H^+ + 2e^- \rightarrow H_2$	−0.8	−0.8	−0.8	−0.5	−0.6	−0.6	−0.6
6[d]								+0.3

[a] From cyclic voltammograms at scan rates of 100 or 200 mV s^{-1}. [b] A quasireversible couple appeared at low current at −1.80 and −1.53 V which is assigned to an unknown impurity. [c] Assignment of this oxidation wave is tentative due to low current density and/or a sensitivity to exact experimental conditions. [d] Observed as a consequence of 4′; redox process is unknown.

Table II. Summary of Redox Processes Occurring in Solutions of $[M^VO(XR)_4]^-$ and $[M_2O_2(XR)_6Z]^-$ in DMF and MeCN

peak no.[a]	redox process	comments
7,7′	$[M^VO(XR)_4]^- + e^- \rightleftharpoons [M^{IV}O(XR)_4]^{2-}$	couple A
8	$[M^V_2O_2(XR)_6Z]^- + 2e^- \rightarrow [M^{IV}O(XR)_4]^{2-} +$ "Mo^{IV}"	nature of "Mo^{IV}" is not known
9,9′	$[M^V_2O_2(XR)_6Z]^- + e^- \rightleftharpoons [M^{IV},V_2O_2(XR)_6Z]^{2-}$	couple B: 9 corresponds to transfer of the first electron in 8; most clearly seen for $[Mo_2O_2(SePh)_6(OMe)]^-$
10,10′	$[M^{IV},V_2O_2(XR)_6Z]^{2-} + e^- \rightleftharpoons [M^{IV}_2O_2(XR)_6Z]^{3-}$	10′ detected only at low temperatures and very fast scan rates
11,11′	$[M^{VI}O(XR)_4] + e^- \rightleftharpoons [M^VO(XR)_4]^-$	couple D: seen for M = W; 11′ is the first step of process E
12′	Ox of ligand XR^- from $[M^V_2O_2(XR)_6Z]^-$?	see Figure 6b
13′	Ox of ligand XR^- from unknown metal species?	see Figure 6b

[a] Primes indicate oxidative processes.

platinum electrode, and controlled-potential electrolysis (CPE) at a platinum electrode, coupled with coulometry and dc polarographic monitoring of the products of electrolysis. The experiments employed were carried out on a Princeton Applied Research Corp. Model 170 instrument. All solutions were flushed with purified, solvent-saturated argon prior to obtaining data. Low temperatures were attained via suitable slush baths and the temperature was monitored inside the cell. Cyclic voltammetry at fast scan rates employed an oscilloscope and transient recorder (Datalab DL901) for data accumulation. An inlaid platinum disk (Beckman 39002A5) or platinum-wire working electrode was employed. The reference electrodes were $Ag/AgNO_3$ (0.1 M) for MeCN and the standard calomel electrode (SCE, PAR 9331) for DMF solutions. Each reference electrode was incorporated into a Luggin capillary containing supporting electrolyte and solvent to minimize Ag^+ or H_2O contamination of the solution. The coulometric cell was adapted from that described by ref 17. Analytical grade dimethylformamide (DMF) was treated[18] with molecular sieves and BaO, twice fractionally distilled under dinitrogen at less than 15 mmHg pressure, and stored in the dark at 5 °C. Analytical grade acetonitrile (MeCN) was further purified according to ref 19. $Et_4N[PF_6]$ (Southwestern Analytical Chemistry) was dried at 110 °C in vacuum and employed as the supporting electrolyte (0.1 M).

Results

Ligand Species. As the thiolate and selenolate ligand species are themselves electroactive, their voltammetric properties at Pt electrodes in DMF and MeCN solution were defined. This work extends previous studies[20] of HSPh–PhSSPh in DMF and PhSSPh in MeCN. Solutions of the thiols HSR, thiolate salts $NEt_4[SR]$, and disulfides RSSR (R = Ph, *p*-tolyl, CH_2Ph) as well as HSePh and PhSeSePh were systematically examined. Assignment of the redox processes observed is made in Table I and typical cyclic voltammograms are shown in Figure 1.

Several observations can be made.

(1) The redox processes are highly irreversible. Processes 1 and 2 cannot be individually resolved for XR = SCH_2Ph and SePh, and the relative peak positions for 1′ and 2′ invert from XR = SPh to XR = SePh.

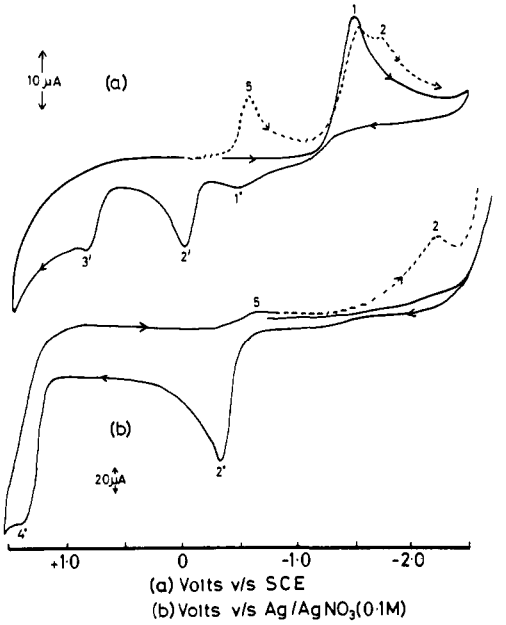

Figure 1. Cyclic voltammograms for 10^{-3} M solutions of (a) HSPh in DMF (scan rate 200 mV s^{-1}) and (b) $[Et_4N]SPh$ in MeCN (scan rate 500 mV s^{-1}): (—), initial scan; (---), second scan. See Table I for identification of the redox processes associated with the peak numbers.

(2) Peak currents and potentials for processes 1, 1′, 3′, and 5 vary appreciably with the exact conditions of observation, a phenomenon often associated with processes involving hydrogen-based species and adsorption phenomena.[21]

(3) The adsorption-controlled version of process 1 (XR = SPh) in DMF seen previously[20b] was not detected in the present study.

(4) The prominent oxidation peak 4′ observed near the solvent limit (Figure 1b) is assigned to the one-electron oxidation of RXXR. However, the overall process is a multielectron one[20a,22]

(17) Rigdon, L. P.; Harrer, J. E. *Anal. Chem.* **1974**, *46*, 696–700.
(18) Juillard, J. *Pure Appl. Chem.* **1979**, *49*, 885–892.
(19) Walter, M.; Ramaley, L. *Anal. Chem.* **1973**, *45*, 165–166.
(20) (a) Bontempelli, G.; Magno, F.; Mazzochin, G.-A. *J. Electroanal. Chem. Interfacial Electrochem.* **1973**, *42*, 57–67. (b) Magno, F.; Bontempelli, G.; Pilloni, G. *Ibid.* **1971**, *30*, 375–383.
(21) Adams, R. N. "Electrochemistry at Solid Electrodes"; Marcel Dekker: New York, 1969.
(22) Howie, J. K.; Houts, J. J.; Sawyer, D. T. *J. Am. Chem. Soc.* **1977**, *99*, 6323–6326.
(23) Nicholson, R. S. *Anal. Chem.* **1966**, *38*, 1406.

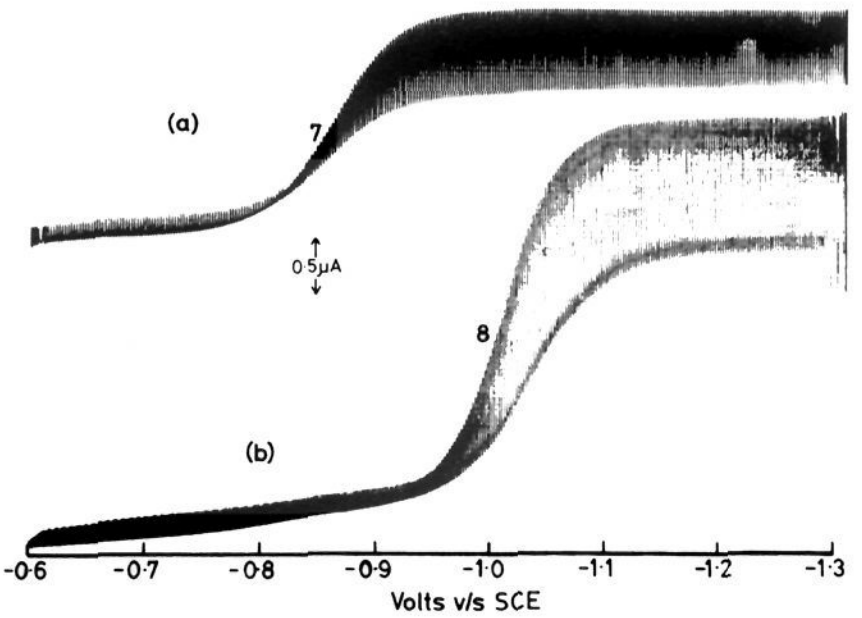

Figure 2. Direct current polarograms (drop time, 0.5 s) of 8.5×10^{-4} M solutions in DMF of (a) $Et_4N[MoO(S\text{-}p\text{-tolyl})_4]$ and (b) $Et_4N[Mo_2O_2(S\text{-}p\text{-tolyl})_6(OMe)]$.

Table III. dc Polarography and Coulometry Data for the Reduction Processes 7 and 8 in DMF and MeCN

solvent	anion[a]	$E_{1/2}$, V	$E_{3/4} - E_{1/4}$[c]	n[d]
DMF	$[MoO(SPh)_4]^-$	−0.82	56	0.86
	$[MoO(S\text{-}p\text{-tolyl})_4]^-$	−0.87	59	0.92
	$[MoO(SCH_2Ph)_4]^-$ [b]	−0.9		
	$[Mo_2O_2(SPh)_6(OMe)]^-$	−0.91	58	2.0
	$[Mo_2O_2(SPh)_6(OEt)]^-$	−0.93	73	
	$[Mo_2O_2(S\text{-}p\text{-tolyl})_6(OMe)]^-$	−1.02	52	2.0
	$[Mo_2O_2(SCH_2Ph)_7]^-$	−1.05	54	
	$[MoO(SePh)_4]^-$	−0.78	58	
	$[Mo_2O_2(SePh)_6(OMe)]^-$	−0.95	59	1.8
	$[WO(SPh)_4]^-$ [b]	−1.1		0.95
	$[W_2O_2(S\text{-}p\text{-tolyl})_6(OMe)]^-$	−1.44	35	2.0
	$[WO(SePh)_4]^-$	−0.94	62	
	$[W_2O_2(SePh)_6(OMe)]^-$	−1.15	38	
MeCN	$[MoO(SPh)_4]^-$	−1.13	71	
	$[MoO(S\text{-}p\text{-tolyl})_4]^-$	−1.18	58	
	$[MoO(SCH_2Ph)_4]^-$ [b]	−1.2		
	$[Mo_2O_2(SPh)_6(OMe)]^-$	−1.26	62	
	$[Mo_2O_2(SPh)_6(OEt)]^-$	−1.27	123	
	$[Mo_2O_2(S\text{-}p\text{-tolyl})_6(OMe)]^-$	−1.34	58	
	$[Mo_2O_2(SCH_2Ph)_7]^-$	−1.34	58	

[a] 10^{-3} M solutions of the Et_4N^+ salts at 25 °C; drop time 1 s. [b] Calculated as the potential[23] at 0.8517 I_{pc} in the cyclic voltammogram at 25 °C. [c] Units are in mV. [d] n is the number of electrons per molecule.

as the product radical cation reacts with the solvent, supporting electrolyte, or residual water with production of protons (detected by process 5; see Figure 1b).

A knowledge of these free-ligand processes is most important in properly assigning the electron-transfer processes of the metal complexes. In addition, ligand-based products appear as a consequence of chemical reactions subsequent to such electron transfer or as a consequence of nonelectrochemical phenomena. In the latter context, for example, the mononuclear species I are rather sensitive to traces of dioxygen and/or protonic impurities in solution, and the initial cathodic scan of fresh solutions often shows the presence of HXR, detected by process 1. The binuclear species II are less sensitive to the impurities. A summary of the redox processes observed for the metal complexes is given in Table II.

Reductive Processes. (i) Mononuclear Species I. The first reduction process (7) was studied by dc polarography (Table III, Figure 2a) and cyclic voltammetry (CV) (Table IV, Figure 3). For $[MO(SR)_4]^-$ at low temperatures (−40 to −60 °C), this reduction process satisfies the essential criteria[24] for a chemically reversible electron-transfer process (e.g., see Table IV). At 25 °C, the electron-transfer step at the dme is reversible, while at platinum it is quasireversible for all species I.

Controlled-potential electrolysis (CPE) coupled with coulometry in DMF at 25 °C (Table III) suggests[25] a one-electron process.

(24) Brown, E. R.; Lange, R. F. *Tech. Chem.* (*N.Y.*) **1971**, *1*, 433–457.

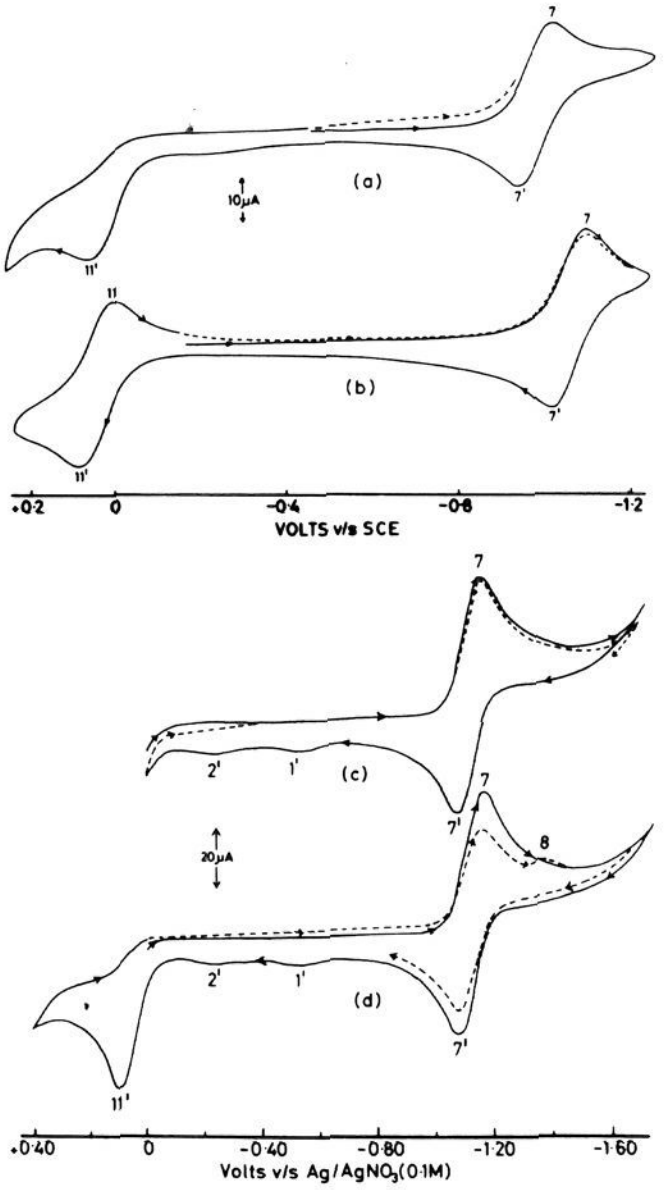

Figure 3. Cyclic voltammograms (scan rate, 200 mV s^{-1}) of (a) 3×10^{-3} M $Et_4N[WO(SPh)_4]$ in DMF at 25 °C, (b) same solution at −40 °C, (c) 8×10^{-3} M $Et_4N[MoO(SPh)_4]$ in MeCN at 25 °C, and (d) same solution *including* peak 11′.

Table IV. Cyclic Voltammetry Data for $[WO(SPh)_4]^-$ in DMF at −20 °C[a]

Couple A(7,7′)

ν	E_{pc}	E_{pa}	ΔE_p	$I_{pc}\nu^{-1/2}c^{-1}$	$I_{pa}I_{pc}^{-1}$
20	−0.950	−0.891	59	0.559	0.99
50	−0.952	−0.889	63	0.542	1.05
100	−0.948	−0.888	60	0.530	1.06
200	−0.962	−0.886	76	0.519	1.03
500	−0.966	−0.881	85	0.492	1.06

Couple D(11,11′)

ν	E_{pc}	E_{pa}	ΔE_p	$I_{pc}\nu^{-1/2}c^{-1}$	$I_{pc}I_{pa}^{-1}$
20	−0.06	+0.012	~70	0.56	0.03
50	−0.061	+0.020	81	0.533	0.57
100	−0.063	+0.023	86	0.513	0.68
200	−0.066	+0.036	102	0.471	0.78
500	−0.062	+0.073	135	0.447	0.93

[a] Units: ν, mV s^{-1}; E_{pc}, V; E_{pa}, V; ΔE_p, mV; $I_{pc}\nu^{-1/2}c^{-1}$, μ A $s^{1/2}$ $V^{-1/2}$ mM^{-1}; $I_{pa}\nu^{-1/2}c^{-1}$, μ A $s^{1/2}$ $V^{-1/2}$ mM^{-1}.

(25) The mononuclear species are rather reactive in solution. Long time scale experiments are particularly difficult for $[MoO(SePh)_4]^-$. The n values derived from controlled-potential electrolysis and coulometry are always less than unity. Spectrophotometric analysis (employing the intense absorption at 598 nm[4]) of an identical solution of $Et_4N[MoO(SPh)_4]$ exposed to the handling conditions of the electrolysis indicated 15% decomposition over 30 min (via O_2 and/or protonic impurity scavenging). In these circumstances, the inference of a one-electron step for an n value greater than 0.8 is not unreasonable.

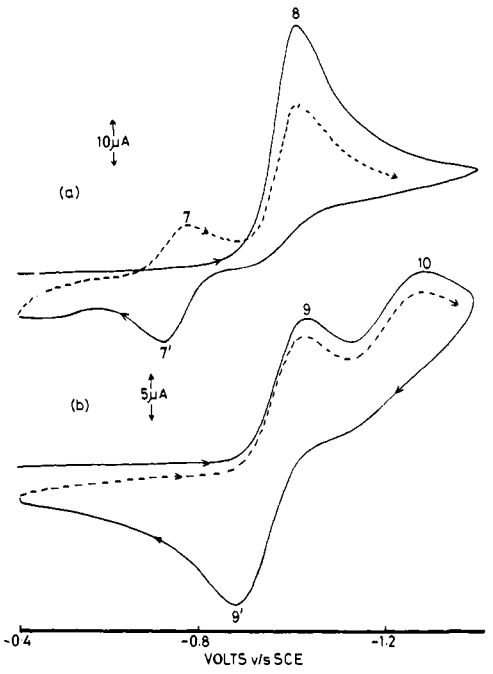

Figure 4. Cyclic voltammograms for 3×10^{-3} M $Et_4N[Mo_2O_2(SePh)_6(OMe)]$ in DMF: (a) at 25 °C and scan rate of 100 mV s^{-1} and (b) at −60 °C and scan rate of 500 mV s^{-1}.

Polarographic monitoring of the products of electrolysis revealed *oxidation* waves at the potentials expected (Table III) if $[M^{IV}O(XR)_4]^{2-}$ is formed via the electrolysis. The data indicate a chemically-reversible couple A.

$$\underset{\text{I}}{[M^{V}O(XR)_4]^{-}} + e^{-} \underset{7'}{\overset{7}{\rightleftharpoons}} [M^{IV}O(XR)_4]^{2-} \qquad \text{(A)}$$

(ii) Binuclear Species II. The triply bridged anions exhibit an irreversible reduction process (8) at 25 °C (Table III, Figures 2b and 4a). The ratio of the polarographic limiting currents associated with processes 7 and 8 for equimolar solutions of I and II is 2.0 ± 0.2 (Figure 2), suggesting a one-electron/metal atom reduction in each case. Coulometry confirms that 8 is a two-electron process (Table III). The dc polarograms of the products of electrolysis of $[Mo_2O_2(SPh)_6(OMe)]^{-}$ are characteristic of $[MoO(SPh)_4]^{-/2-}$ (couple A), and diffusion-controlled limiting currents per unit concentration indicate that *one* molecule of $[Mo^{IV}O(SPh)_4]^{2-}$ is formed per molecule of $[Mo^{V}_2O_2(SPh)_6(OMe)]^{-}$ reduced.

For all the systems II at 25 °C, CV confirms the production of mononuclear species $[M^{IV}O(XR)_4]^{2-}$ (as a consequence of the two-electron process 8) by observation of the secondary peaks 7′ and 7 associated with couple A (e.g., Figure 4a). The chemical reaction which follows electron transfer can be suppressed by effectively shortening the time scale of the experiment and lowering the temperature. Thus, at −60 °C and at scan rates $v \geq 500$ mV s^{-1}, the secondary couple A is eliminated (Figure 4b). In addition, for $[Mo_2O_2(SePh)_6(OMe)]^{-}$, peak 8 resolves into two components 9 and 10 (Figure 4b). Peaks 9 and 9′ form a quasireversible couple (Table V) and quantitative comparisons of the current function $I_{pc}v^{-1/2}c^{-1}$ with those for couple A under similar conditions (e.g., compare Table IV) suggest a one-electron couple.

$$[Mo^{V}_2O_2(SePh)_6(OMe)]^{-} + e^{-} \underset{9'}{\overset{9}{\rightleftharpoons}} [Mo^{V,IV}_2O_2(SePh)_6(OMe)]^{2-} \qquad \text{(B)}$$

Peak 10 is then logically assigned to the process

$$[Mo^{V,IV}_2O_2(SePh)_6(OMe)]^{2-} + e^{-} \xrightarrow{10} [Mo^{IV}_2O_2(SePh)_6(OMe)]^{3-} \qquad \text{(C)}$$

The behavior of the other binuclear species II at low temperature is less clear cut, but, in each case, an oxidation process assignable to 9′ appears. For $[Mo_2O_2(SR)_6(OMe)]^{-}$, 9 and 10 are not quite resolved (see ref 5) at −39 °C in MeCN. However, at very fast scan rates (20000 mV s^{-1}) the oxidative component 10′ of the couple equivalent to C appears to contribute to the measured response.

Table V. Cyclic Voltammetry Data for Couple B(9,9′) of $[Mo_2O_2(SePh)_6(OMe)]^{-}$ at −50 °C in DMF

v	E_{pc}	E_{pa}	ΔE_p	$I_{pc}v^{-1/2}c^{-1}$	$I_{pa}I_{pc}^{-1}$
20	−0.999	−0.929	70	0.547	1.01
50	−1.000	−0.930	70	0.524	1.01
100	−1.007	−0.921	86	0.488	1.11
200	−1.017	−0.915	102	0.442	1.08
500	−1.025	−0.912	113	0.428	1.09

[a] Units: v, mV s^{-1}; E_{pc}, V; E_{pa}, V; ΔE_p, mV; $I_{pc}v^{-1/2}c^{-1}$, μ A $s^{1/2}$ $V^{-1/2}$ mM^{-1}.

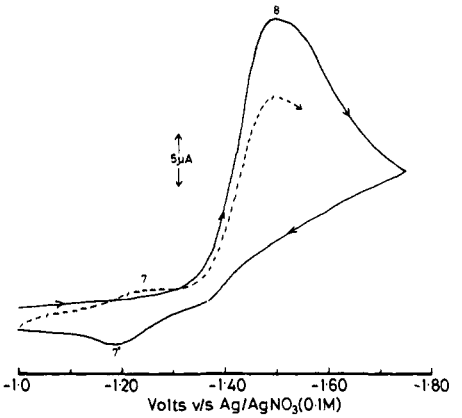

Figure 5. Cyclic voltammogram for 10^{-3} M $Ph_4As[Mo_2O_2(SCH_2Ph)_7]$ in MeCN at 25 °C and a scan rate of 500 mV s^{-1}.

A CV scan for $[Mo_2O_2(SCH_2Ph)_7]^{-}$ at 25 °C (Figure 5) is qualitatively similar to those of other anions II (Figure 4a). Particularly interesting is the observation of couple A for $[MoO(SCH_2Ph)_4]^{-/2-}$ (Table III).

Oxidative Processes. A primary oxidation process 11′ is seen for all anions I (Figure 3). It is irreversible under all conditions examined for the molybdenum cases, but a reduction component 11 appears at lower temperatures for the tungsten cases. The CV data (Table IV) for $[WO(SPh)_4]^{-}$ in DMF at −20 °C shows that the couple approaches quasireversibility at high scan rates. Comparison of the current function for couples (7,7′) and (11,11′) suggests (Table IV) that both are one-electron processes and that (11,11′) is due to couple D. The current ratio I_{pc}/I_{pa} approaches

$$[W^{VI}O(SPh)_4] + e^{-} \underset{11'}{\overset{11}{\rightleftharpoons}} [W^{V}O(SPh)_4]^{-} \qquad \text{(D)}$$

0 at low scan rates at −20 °C and indicates that the electrochemically generated $[W^{VI}O(SPh)_4]$ is involved in a subsequent chemical reaction. The nature of that reaction is most clearly revealed by study of $[Mo^{V}O(SR)_4]^{-}$ in MeCN at 25 °C. The peak separations of processes 7, 8, 1, and 2 for this system permits their individual detection, and the data suggests assignment of the overall process to (E). The assignment is supported by several

$$2[Mo^{V}O(SR)_4]^{-} \xrightarrow{\text{MeCN}} [Mo^{V}_2O_2(SR)_6(MeCN)] + RSSR + 2e^{-} \qquad \text{(E)}$$

facts. (a) RSSR appeared (detected by peak 2) as a consequence of 11′. (b) A secondary process 8 (Figure 3d) appeared also as a consequence of 11′. The peak is indicative of the two-electron reduction[26] of a triply bridged species (Table III, Figure 4a) at 25 °C. Electrode process 8 is more pronounced the higher the concentrations of $[MoO(SR)_4]^{-}$. Consequently, the production

(26) Existing data suggest that the peak potentials of process 8 of II are essentially independent of the nature of the unique bridging ligand, Z. The triply bridged binuclear product is formulated with MeCN coordinated in position Z as benzene thiolate cannot occupy that position.[16]

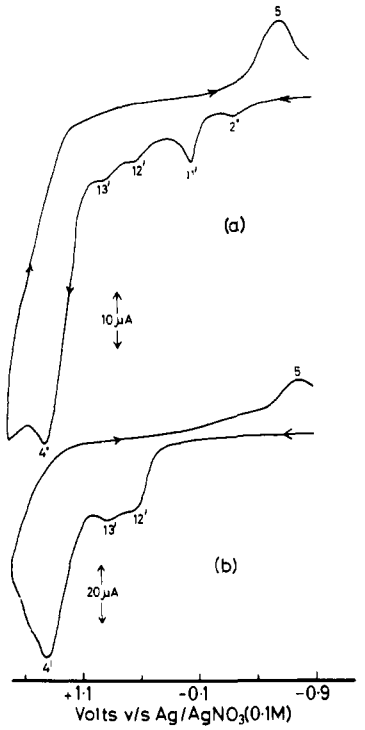

Figure 6. Cyclic voltammograms of 10^{-3} M solutions in MeCN at 25 °C and scan rate of 200 mV s^{-1}: (a) $Et_4N[MoO(SPh)_4]$; (b) $Et_4N[Mo_2O_2(SPh)_6(OMe)]$.

of $[Mo_2O_2(SR)_6(MeCN)]$ must depend upon a second- or higher order process involving reaction of $[Mo^VO(SR)_4]^-$ with mononuclear species formed subsequent to the initial electron-transfer process or via association of such species. Furthermore, the process is kinetically controlled since the peak height of 8 is much lower than predicted for a diffusion-controlled two-electron step. Reasonable mechanisms for the formation of $[Mo_2O_2(SR)_6(MeCN)]$ dependent upon the initial oxidation process 11′

$$[Mo^VO(SR)_4]^- \xrightarrow{11'} [Mo^{VI}O(SR)_4] + e^-$$

are presented in the scheme of eq F1–F3 (where coordinating

$$[Mo^{VI}O(SR)_4] \rightarrow [Mo^VO(SR)_3] + SR\cdot$$

$$[Mo^VO(SR)_3] + [Mo^VO(SR)_4]^- \xrightarrow{\text{slow}} [Mo^V_2O_2(SR)_6] + SR^-$$

$$SR^- \rightarrow SR\cdot + e^-$$

$$2SR\cdot \rightarrow RSSR \qquad \text{(F1)}$$

$$[Mo^{VI}O(SR)_4] \rightarrow [Mo^{IV}O(SR)_2] + RSSR$$

$$[Mo^{IV}O(SR)_2] + [Mo^VO(SR)_4]^- \xrightarrow{\text{slow}} [Mo^{V,IV}_2O_2(SR)_6]^-$$

$$[Mo^{V,IV}_2O_2(SR)_6]^- \rightarrow [Mo^V_2O_2(SR)_6] + e^- \qquad \text{(F2)}$$

$$[Mo^{IV}O(SR)_2] + [Mo^{VI}O(SR)_4] \xrightarrow{\text{slow}} [Mo_2O_2(SR)_6] \qquad \text{(F3)}$$

MeCN is ignored for simplicity of presentation). Discrimination between these mechanisms must await direct detection of the various intermediates.

(c) Oxidation peaks 12′ and 13′ were observed at potentials more positive than that for 11′ (Figure 6a). These are assigned to processes involving a triply bridged binuclear species by comparison with the behavior of $[Mo^V_2O_2(SR)_6Z]^-$ (Figure 6b). They probably involve oxidation of ligand thiolate (with a $Mo^{VI,V}_2$ intermediate?) from the binuclear species and lead to the appearance of protons in solution (detected by peak 5).

(d) A similar oxidation was observed occurring when $FeCl_3$ reacts[16] with $[MoO(SR)_4]^-$ as in eq G. Oxidation and removal

$$2[Mo^VO(SR)_4]^- + Fe^{III}Cl_3 \xrightarrow{MeCN} [Mo^V_2O_2(SR)_6Cl]^- + Fe^{II}Cl_2 + {}^1/_2RSSR + RS^- \qquad \text{(G)}$$

Scheme I. Redox Interconversions:* $n = 1$ for Z = $[OR']^-$, $[NR'_2]^-$, Cl; $n = 0$ for Z = MeCN, DMF

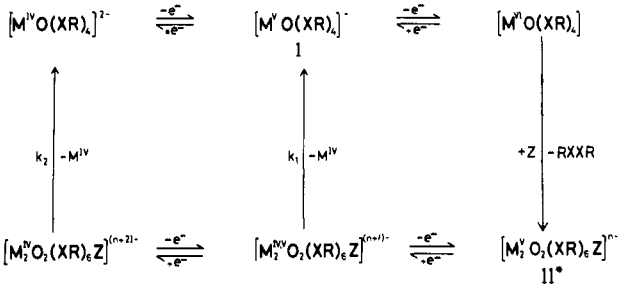

of one of the ligands apparently deprives $[MoO(SR)_4]^-$ (R = aryl) of its sterically controlled kinetic stability.

Discussion

The essential redox processes observed in this work are summarized in Table II and Scheme I. Interconversion of the mononuclear and triply bridged binuclear species occurs via redox processes which can be considered to involve both the metal and ligand centers. The availability of complete sets of molybdenum and tungsten thiolate and selenolate species I and II has been crucial to a detailed understanding of these redox processes.

The mononuclear anions I are reversibly reduced to M^{IV} dianions, and similar behavior is observed[14,27] for certain other oxomolybdenum(V) species. On the other hand, the reduction behavior of the triply bridged anions II is more complex.

For short time scale experiments (faster scan rates, lower temperatures), the electron transfer can outrun subsequent chemical reactions, and cycling between II and its one- and two-electron reduction products $M^{V,IV}_2$ and M^{IV}_2 is important. For longer time scales (slower scan rates, higher temperatures), $M^{V,IV}_2$ and M^{IV}_2 each react (rate constants k_1 and k_2 of Scheme I) and $[M^{IV}O(XR)_4]^{2-}$ is a product in each case. The contribution of each reaction pathway will be governed by the relative magnitudes of k_1 and k_2 for the given set of conditions. At 25 °C reaction via $M^{V,IV}_2$ predominates. Note that both pathways lead to the formation of one molecule of $[M^{IV}O(XR)_4]^{2-}$ per two-electron reduction involving one molecule of II. Electroactive species are not formed from the other metal atom and its fate is unknown.

This reduction behavior of species II can be compared to that of the doubly bridged compounds $[Mo^V_2O_2(\mu\text{-}S)_2L_2]$ (L = ethyl cysteinate, diethyl dithiocarbamate) and related species in Me_2SO studied by Schultz and Newton.[10,11] For example, a transition from one- to two-electron behavior is also found[11] for $[Mo_2O_2(\mu\text{-}S)_2(Et_2dtc)_2]$ as the time scale of the experiment is increased at 22 °C (c.f. Figure 4). The primary reduction product $Mo^{IV,V}_2$ undergoes an apparently second-order chemical reaction which yields a species which is further reduced at the potential of the first voltammetric wave. That species could unfortunately not be identified in the doubly bridged systems but is very probably $[M^VO(XR)_4]^-$ in the present triply bridged systems (Scheme I).

The present work also points the way to the observation of alkyl-substituted anions I if the required species II is available. Thus $[MoO(SCH_2Ph)_4]^{-/2-}$ are generated from $[Mo_2O_2(SCH_2Ph)_7]^-$ (Figure 5), and although such alkyl-substituted mononuclear species cannot be isolated in substance at room temperature,[4,16] they are apparently sufficiently long-lived to be observed on the CV time scale at 25 °C. Such species have also been generated chemically at low temperature and detected by ESR spectroscopy.[4]

Chemical reactions follow oxidation of the mononuclear anions I and result in the appearance of oxidized ligand RXXR and the formation of triply bridged binuclear species (Scheme I and eq E and F1–F3). $[W^{VI}O(XR)_4]$ is observed on the CV time scale at lower temperatures, apparently due to the relative slowness of a general intramolecular redox step leading to a coordinatively

(27) Bradbury, J. R.; Wedd, A. G., unpublished observations.

unsaturated M^V or M^{IV} mononuclear species.

$$[M^{VI}O(XR)_4] \rightarrow [M^{V}O(XR)_3] + SR\cdot$$
$$\rightarrow [M^{IV}O(XR)_2] + RSSR$$

Such processes are certainly the source of the general instability of molybdenum(VI) and tungsten(VI) thiolate species. Stable dioxo-molybdenum(VI) complexes containing multidentate ligands feature[28] trans thiolate-sulfur ligand atoms to suppress disulfide elimination. The EXAFS spectrum[3] of such a complex, $[Mo^{VI}O_2[N(CH_2CH_2S)_2(CH_2CH_2SMe)]$, is intriguingly similar to that of the fully oxidized form of sulfite oxidase.

The importance of thiolate ligand redox processes in the present work is mirrored in significant attractive interactions between cis thiolate ligands in $(Me_4N)_2[Mo^{V}_2O_4(SPh)_4]$[29] and those in $[Mo^{VI}O_2(SC(CH_3)_2CH_2NHCH_3)_2]$.[30] Besides the possibility of such interactions modulating the catalytic properties of molybdenum centers, cysteinate ligand redox processes might be considered in a detailed examination of electron transfer in molybdo enzymes. In the resting II inactive form of xanthine oxidase, electron spin-spin coupling is observed[31] between Mo and Fe_2S_2 which constitutes part of the internal electron-transfer chain. The two centers may be separated by a distance (present estimates[31b] suggest 8-13 Å) which might eliminate a direct low activation energy electron-transfer pathway via Mo and Fe cysteinate ligands. However, involvement of cysteinate ligands (or the recently discovered[32] pteridine unit) would significantly reduce the distance over which electron-transfer mechanisms such as electron channeling or quantum mechanical tunneling would need to operate.

In the present work, the mononuclear-binuclear interconversions appear to be driven by the thermodynamic instability of (a) the metal oxidation state VI relative to V and IV in the presence of the redox-active XR^- ligands, (b) the $M^V(d^1)$ mononuclear species relative to M^V_2 binuclear species which are certainly stabilized[16] by intermetallic bonding, and (c) the $M^{IV,V}_2$ and M^{IV}_2 binuclear species relative to $M^{IV}(d^2)$ mononuclear species assumed to have low-spin d_{xy}-based ground states (apparently addition of electrons to the spin-coupled species II requires occupation of antibonding levels).

However, examples of mononuclear M^{VI} and M^V and binuclear $M^{IV,V}_2$ and M^{IV}_2 are observed as a result of varying degrees of kinetic stability. In this context, $[Mo^{V,IV}_2O_2(SePh)_6(OMe)]^-$ has a significant lifetime at -50 °C in DMF (Figure 4b), and attempts are currently under way to characterize it by ESR spectroscopy.

Acknowledgment. A.G.W. thanks the Australian Research Grants Committee for financial support of this work. J.R.B. acknowledges the award of a Commonwealth Postgraduate Scholarship.

(28) Berg, J. M.; Hodgson, K. O.; Cramer, S. P.; Corbin, J. L.; Elsberry, A.; Pariyadath, N.; Stiefel, E. I. *J. Am. Chem. Soc.* **1979**, *101*, 2776-2779.
(29) Dance, I. G.; Wedd, A. G.; Boyd, I. W. *Aust. J. Chem.* **1978**, *31*, 519-526.
(30) Stiefel, E. I.; Miller, K. F.; Bruce, A. E.; Corbin, J. L.; Berg, J. M.; Hodgson, K. O. *J. Am. Chem. Soc.* **1980**, *102*, 3624-3626.
(31) (a) Lowe, D. J.; Bray, R. C. *Biochem. J.* **1978**, *169*, 471-479. (b) Coffman, R. E.; Buettner, G. R. *J. Phys. Chem.* **1979**, *83*, 2392-2400.
(32) Johnson, J. L.; Hainline, B. E.; Rajagopalan, K. V. *J. Biol. Chem.* **1980**, *255*, 1783-1786.

Reaction of Fluoroxysulfate with Aromatic Compounds[1a]

Dominic P. Ip, Carol D. Arthur,[1b] Randall E. Winans, and Evan H. Appelman*

Contribution from the Chemistry Division, Argonne National Laboratory, 9700 South Cass Avenue, Argonne, Illinois 60439. *Received June 23, 1980*

Abstract: The fluoroxysulfate ion, SO_4F^-, substitutes fluorine on aromatic compounds in acetonitrile solution at room temperature. However, benzyl fluoride is the principal product from toluene. Other products are also formed, particularly in the case of the less reactive aromatic substrates. Product distributions and relative reactivities are interpreted in terms of an initial electrophilic attack that can be followed by free-radical side reactions.

Introduction

It is rather uncommon to find a reagent that will substitute fluorine for aromatic hydrogen. Molecular fluorine itself tends to add to aromatics,[2,3] although substitution can be achieved under carefully controlled conditions.[3,4] Trifluoromethyl hypofluorite, CF_3OF, only effects clean substitution by means of low-temperature photolysis[5] or in reactions with activated aromatic substrates.[6] Xenon difluoride has been found to produce fluoroaromatics in good yield in the presence of HF as a catalyst,[7] but it is an inherently costly reagent. A very recent publication reports fluorination of aromatics by AgF_2.[8]

The fluoroxysulfate ion, SO_4F^-, has recently been prepared in our laboratory.[9] It is the first ionic hypofluorite to be isolated, and our preliminary results suggested that it might, in fact, react with aromatic compounds as an electrophilic fluorinating agent. Unlike many powerful fluorinating agents, the cesium and rubidium fluoroxysulfate salts are relatively stable compounds that are easy to prepare, store, and use. Because of this, they could have potential application as synthetic reagents for organic chemistry. We have therefore undertaken to study in some detail the reactions of fluoroxysulfate with a variety of aromatic species.

Acetonitrile was found to be a suitable solvent for these reactions. Cesium and rubidium fluoroxysulfates are soluble in

(1) (a) Work performed under the auspices of the Office of Basic Energy Sciencies, Division of Chemical Sciences, U.S. Department of Energy. (b) Undergraduate Research Participant, 1979, supported by the Argonne Center for Educational Affairs.
(2) Grakauskas, V. *J. Org. Chem.* **1969**, *34*, 2835.
(3) Grakauskas, V. *J. Org. Chem.* **1970**, *35*, 723.
(4) Cacace, F.; Giacomello, P.; Wolf, A. P. *J. Am. Chem. Soc.* **1980**, *102*, 3511.
(5) Kollonitsch, J.; Barash, L.; Doldouras, G. A. *J. Am. Chem. Soc.* **1970**, *92*, 7494.
(6) Barton, D. H. R.; Ganguly, A. K.; Hesse, R. H.; Loo, S. N.; Pechet, M. M. *J. Chem. Soc., Chem. Commun.* **1968**, 806.
(7) Shaw, M. J.; Hyman, H. H.; Filler, R. *J. Am. Chem. Soc.* **1970**, *92*, 6498.
(8) Zweig, A.; Fischer, R. G.; Lancaster, J. E. *J. Org. Chem.* **1980**, *45*, 3597.
(9) Appelman, E. H.; Basile, L. J.; Thompson, R. C. *J. Am. Chem. Soc.* **1979**, *101*, 3384.

0002-7863/81/1503-1964$01.25/0